The effects of monocytes on tumor cell extravasation in a 3D vascularized microfluidic model

A. Boussommier-Calleja [a], Y. Atiyas [b], K. Haase [a], M. Headley [c, d], C. Lewis [e], R.D. Kamm [a, b, *]

[a] Mechanical Engineering, Massachussetts Institute of Technology, USA
[b] Biological Engineering, Massachussetts Institute of Technology, USA
[c] Department of Pathology, University of California, San Francisco, CA, USA
[d] Clinical Research Division, Fred Hutchinson Cancer Research Center, Seattle, WA, USA
[e] Department of Oncology & Metabolism, University of Sheffield, UK

ARTICLE INFO

ABSTRACT

Metastasis is the leading cause of cancer-related deaths. Recent developments in cancer immunotherapy have shown exciting therapeutic promise for metastatic patients. While most therapies target T cells, other immune cells, such as monocytes, hold great promise for therapeutic intervention. In our study, we provide primary evidence of direct engagement between human monocytes and tumor cells in a 3D vascularized microfluidic model. We first characterize the novel application of our model to investigate and visualize at high resolution the evolution of monocytes as they migrate from the intravascular to the extravascular micro-environment. We also demonstrate their differentiation into macrophages in our all-human model. Our model replicates physiological differences between different monocyte subsets. In particular, we report that inflammatory, but not patrolling, monocytes rely on actomyosin based motility. Finally, we exploit this platform to study the effect of monocytes, at different stages of their life cycle, on cancer cell extravasation. Our data demonstrates that monocytes can directly reduce cancer cell extravasation in a non-contact dependent manner. In contrast, we see little effect of monocytes on cancer cell extravasation once monocytes transmigrate through the vasculature and are macrophage-like. Taken together, our study brings novel insight into the role of monocytes in cancer cell extravasation, which is an important step in the metastatic cascade. These findings establish our microfluidic platform as a powerful tool to investigate the characteristics and function of monocytes and monocyte-derived macrophages in normal and diseased states. We propose that monocyte-cancer cell interactions could be targeted to potentiate the anti-metastatic effect we observe in vitro, possibly expanding the milieu of immunotherapies available to tame metastasis.

1. Introduction

Monocytes have long been considered merely as precursors to macrophages or dendritic cells. However, recent accounts in immune-oncology, allergic disease, and liver injury among others, have established monocytes as effector cells in their own right [1–3]. Monocytes are produced in the bone marrow, continuously circulate in the blood stream, are rapid producers of cytokines and chemokines, and can transmigrate through the vessel wall into the surrounding tissue to become macrophages or dendritic cells [4]. Different types of monocytes exist with specialized functions. In humans, inflammatory or classical monocytes ($CD14^+CD16^-$) are the best studied [5] and are thought to be precursor to macrophages, dendritic cells and other monocyte subpopulations [6,7]. Intermediate monocytes ($CD14++CD16^+$), are a more differentiated subset and are highly phagocytic [8]. Lastly, patrolling or non-classical monocytes ($CD14-CD16^+$) act as vascular scavengers, clearing vascular debris such as dying endothelium or cholesterol [9]. This heterogeneity has raised many questions about their role in normal and diseased states, and has created a need for high-throughput physiological models to study them in-depth across the entire spectrum of their function and differentiation. In parallel,

* Corresponding author. 500 Technology Square, 02139 Cambridge, MA, USA.
E-mail address: rdkamm@mit.edu (R.D. Kamm).

the recent success of cancer immunotherapy has uncovered the tremendous therapeutic potential that manipulating immune cells offers. While many studies have focused on targeting T cells for treating cancer [10], other immune cells that hold much promise, such as monocytes, have been less investigated. Within the immune system, monocytes are uniquely positioned to be targeted because they are a population of highly heterogeneous and plastic cells that continuously respond and adapt to their microenvironment's needs and can be triggered to variably promote or regulate inflammation. Thus, understanding the mechanisms controlling monocyte dynamic heterogeneity could form the basis for immunotherapy treatments that modulate monocytes towards a phenotype that can help curb a broad set of diseases [11].

Additionally, immune cells are particularly interesting therapeutic targets because they have been shown to play central roles in many diseases, such as cancer [12]. In the context of cancer, studies have investigated more extensively the role of macrophages than monocytes. In primary tumors, macrophages are known to promote cancer cell invasion and intravasation [13,14]. In contrast, fewer studies examine the role of macrophages in metastasis, and even less that of undifferentiated monocytes. It has been shown that depletion of macrophages decreases cancer cell extravasation in murine lungs [15], suggesting that macrophages directly help cancer cell extravasation. Several studies have now shown that macrophages help with cancer cell survival, seeding and proliferation following their extravasation in a new tissue [16–19]. Only recent studies have examined whether monocytes have an impact on cancer progression prior to their differentiation into macrophages [1,20]. Interestingly, these studies have suggested that different monocyte subpopulations behave differently in cancer metastasis. Patrolling monocytes have been shown to reduce metastasis by scavenging tumor material and promoting natural killer cell recruitment and activation [1]. Inflammatory monocytes have been shown to potentially facilitate cancer cell extravasation and their engraftment by replenishing the pool of macrophages present at the secondary site of tumor formation [20,21]. However, these studies did not study direct engagement between inflammatory monocytes and tumor cells but rather the effects of monocytes after they had been recruited to the metastatic site. Thus, there is a need to understand whether monocytes can directly affect tumor cells prior to their trans-endothelial migration and differentiation.

Intravital imaging has brought unprecedented insight into the role of immune cells in tissue homeostasis and cancer [13,22]. However, it requires specialized equipment and training, and relies on animal use. We have established microfluidic devices as a unique and powerful platform for studying immune and cancer cell dynamics, in particular during the metastatic cascade [23]. Microfluidic devices, are inexpensive to produce, and minimize both reagent and cell use by utilizing precision channels ranging from 10 to 100 μm [24]. In particular, they offer unhindered access for high-resolution imaging, enabling single cell analysis with high temporal acuity [25]. Our laboratory [26] and others [27] have developed methodology allowing the formation of complex and perfusable vascular networks within these microfluidic channels. Importantly, by introducing monocytes and cancer cells into the microvessels, we can continuously monitor transit between the intra- and extra-vascular compartments, as previously done to study tumor cell trans-endothelial migration [28].

In this study, we employ a 3D microfluidic model to study intravascular migration, transmigration and differentiation of monocytes through human microvasculature. We investigate the differential physiology of monocytes between vascular compartments and the contrasting effects of monocytes before and after their trans-endothelial migration on tumor cell extravasation.

Importantly, we demonstrate the first true high-resolution visualization of monocyte transmigration through human vasculature. Our platform replicates physiologic differences between inflammatory and patrolling monocytes extravasation patterns, as previously observed in vivo. Our results suggest that inflammatory monocytes largely use myosin IIA to migrate intravascularly, while patrolling monocytes do not. In addition, we demonstrate that, after extravasation, inflammatory monocytes become macrophage-like. Finally, we show that tumor cell extravasation is affected by intravascular monocytes, i.e. before they transmigrate through the endothelium to become macrophage-like. Our novel findings point to an effect of monocytes on cancer cell metastatic progression as of yet unknown that offers specific therapeutic opportunity, in particular for cancer immunotherapy.

2. Material and methods

2.1. Cells and reagents

Cytoplasm-labelled GFP-endothelial cells (HUVECs) were obtained from Angio-proteomie. Normal human lung fibroblasts were obtained from Lonza and tagged fluorescently with tdTomato for selected experiments. Monocytes were isolated from human blood (see next section). EGM-2 and FGM-3 (Lonza) media was used to maintain HUVECs and fibroblasts in culture. MDA-MB-231 (human breast cancer cell line) and MDA-MB-435 (human melanoma cancer cell line) were obtained from Lonza, tagged fluorescently with tdTomato, and maintained in DMEM + 10% FBS (Life Technologies) + 1% Penicillin-Streptomyocin (Life Technologies). Antibodies (and their corresponding isotype controls) for FACs experiments were obtained from Biolegend (anti human PE anti-CD68, FITC anti- CD163, PE anti- CD206, PE anti-CCR2), eBiosciences (anti- CD14 eFluor 450), Miltenyi Biotec (anti-CD16) and Abcam (PE anti-myosin IIA). For immunostaining, we used a rabbit anti-CD206 antibody (Abcam), or an anti-myosin IIA antibody (Abcam).

2.2. Monocyte isolation from blood

Monocytes were isolated from human blood, freshly withdrawn from 20 healthy volunteer donors (Supplemental Table 1) who all signed a consent form. Blood was obtained in a clinical research center at MIT, following a protocol approved by the Committee on the Use of Humans as Experimental Subjects (COUHES). Our work is in accordance with The Code of Ethics of the World Medical Association. Volunteer's health was determined by a screening survey and health assessment was performed by a research Nurse Practitioner. A volume of 100 ml of blood was quickly diluted with RoboSep (StemCell), layered on a density gradient (Ficoll Paque, GE Healthcare) and centrifuged to obtain the peripheral blood mononuclear cells (PBMCs). The PBMCs were washed several times to minimize platelet contamination. A negative selection cocktail (EasySep™ Human Monocyte Enrichment Kit without CD16 Depletion, StemCell) was used to isolate monocytes from the PBMC mixture.

2.3. Microfluidic device fabrication and microvascular network formation

A PDMS microfluidic device was used for 3D culture of human microvascular networks, as described before [28]. The device is composed of 5 channels, each connected to two 4 mm reservoirs filled with cell media (Fig. 1A). The channels enclose 3 rectangular compartments, connected at each end to a 1 mm opening for introducing the hydrogel-cell mixture. In this study, the hydrogel-
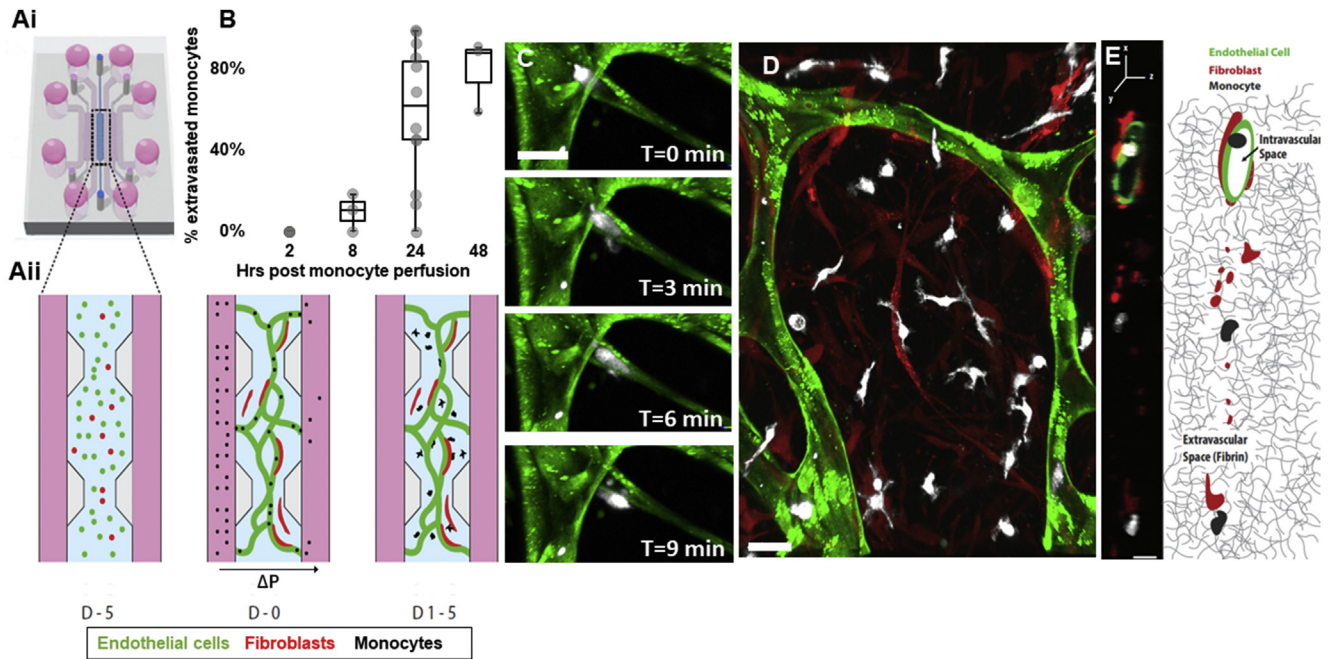
Fig. 1. Monocytes transmigrate through the microvascular network over time. A) i-Schematic of the microfluidic device, showing the central compartment shaded in blue that contains the cells surrounded by the microfluidic channels filled with media (pink). ii- Close-up of the central region containing the cells mixed in a 3D hydrogel at different time points: at day −5, endothelial cells (green) and fibroblasts (red) are suspended in a 3D fibrin gel. 5 days later, at day 0, endothelial cells have connected and formed a network with lumens open to the flanking microfluidic channels. Monocytes are isolated from blood and perfused through the networks thanks to a transient pressure drop (ΔP) established across the central region. Within a few days (D1-5) monocytes have transmigrated through the endothelial wall and are found in the extracellular fibrin gel around the networks, interacting with fibroblasts. B) Quantification of monocyte extravasation 0, 8, 24 and 48 h after monocyte perfusion in the microvascular network. Each data point represents the percentage of extravasated monocyte in one device. N = 3−15 devices per condition, 1−9 donors per condition. C) Confocal images of a monocyte (white) undergoing extravasation through the endothelium (green). Bar is 20 μm. D) Representative image of the monocytes 4 days after perfusion. Most have extravasated and are in the extravascular space, in close interaction with fibroblasts (red). Bar is 20 μm. E) Representative cross-sectional view of a vessel segment (green) and the extravascular space surrounding it, as observed with confocal microscopy and schematically represented (right panel). Fibroblasts (red) are found in the extravascular space within the 3D fibrin matrix, while monocytes (white) can be found either inside the hollow vessels or outside in the 3D fibrin matrix. Bar is 10 μm.

cell mixture was introduced in the central compartment, and the remaining space filled with media. Microvascular networks were formed according to our previously published protocol [26]. Briefly, endothelial cells and fibroblasts were re-suspended in EGM + thrombin at 24×10^6/ml and 6×10^6/ml, respectively. First, HUVECs and fibroblasts were mixed in a 1/1 ratio; they were then mixed with an equal amount of 6 mg/ml fibrin gel, and introduced into the central compartment of the microfluidic device. The final concentration of HUVECs was 6×10^6/ml and 1.5×10^{-6}/ml fibroblasts, in a 3 mg/ml fibrin gel. The reservoirs were filled with EGM-2, which was subsequently changed every day. Over 5 days, endothelial cells self-assembled into a 3D vascular network in the fibrin gel, eventually forming lumens that open to each side of the compartment, towards the microfluidic channels. This provided direct access from the reservoirs, through the microfluidic channel into the vascular network, for cell perfusion (Fig. 1A).

2.4. Monocyte and cancer cell perfusion and imaging

Once monocytes were isolated from blood, they were fluorescently stained with Deep Red Cell tracker (Invitrogen). In order to introduce cells (monocytes or cancer cells) into the microvascular networks, a transient pressure drop was established across the fibrin gel, by filling only the reservoirs to one side of the gel with media containing the cells. Approximately 40000 monocytes were introduced into the reservoir, flowing through the networks at a concentration of 10^6/ml. Monocytes or cancer cells were defined as trapped in the vasculature when their body size was similar to, or smaller than, the vessel diameter, thereby obstructing

the vessel. Alternatively, some monocytes or tumor cells adhered to the vessel wall without obstruction (Fig. S1A). Over time, some of the monocytes extravasated through the endothelial wall into the extracellular space composed of the fibrin gel. Cancer cells were dissociated with trypsin and perfused at 0.4×10^6/ml into the networks. Approximately 20 min after cell delivery, another pressure drop was formed with cell-free media to remove any non-adherent cells from the networks. Note that we saw very little contamination with platelets in our assay which were easily identified because of their much smaller size than monocytes (Fig. S6). On average, the diameters of monocytes, MDA-MB-231 and MDA-MB-435 were 8.7 ± 0.4, 16.3 ± 0.5 and 16.3 ± 1.1 μm, respectively.

The microvascular network was imaged using a confocal microscope (Olympus model FV1000) fit with an environmental chamber to maintain the temperature at 37 °C and appropriate CO_2 and O_2 levels. Devices were typically imaged at 20× (800×800 pixel density) every 1.2 μm of depth, to create a 3D stack of images. The optical resolution was 0.795 μm in the x-y direction. Analyzing cells in 3D at this resolution allowed us to detect whether monocytes were inside or outside of the vessels (Fig. 1B). The interval used for time-lapse imaging ranged from 2 to 20 min intervals, for 0.5−10 h.

2.5. Permeability measurements

To measure permeability, we quantified the diffusion of a fluorescent probe through the vascular network. A larger device (~55 mm³ gel volume) was used to minimize the influence of the probe's diffusion from the microfluidic channel into the fibrin gel. A

similar protocol to that described earlier is used for network formation (using tdTomato-labelled HUVECs from Lonza). At day 7, microvascular networks were perfused with monocytes. Permeability measurements were made by imaging 3 confocal stacks over 5 min intervals following perfusion of 70 kDa FITC dextran through the microvasculature. Post-processing of the volume images was performed using ImageJ. Briefly, projections of the networks were used to generate a perimeter (Pv) differentiating the intra-from the extra-vascular space. This allowed for measurements over the time interval, t, of fluorescence intensity, I, over the total area A_t of the extravascular space, at the first time point (I_{0T}, I_{0v}) and last time point (I_{fT}, I_{fv}) in the extravascular space or inside the vessel, respectively. Assuming that there is no net transfer of fluorophore across the imaging boundary, we can use the following simplified equation to measure permeability, P(cm/s):

$$P(t) = \left(\frac{A_t}{P_v} \left(I_{fT} - I_{0T} \right) \right) \Big/ t \cdot (I_{0v} - I_{0T})$$

2.6. FACs

Flow cytometry was used to characterize monocyte marker expression, using an LSIIR BD Bioscience FACs analyzer. For staining, cells were resuspended in PBS + FBS 2% and first blocked with FcR blocking reagent (Miltenyi Biotec, 1/5 dilution) for 20 min on ice, to avoid non-specific binding. Cells were washed and stained with the antibody of interest for 20 min on ice. For intracellular staining (myosin IIA/CD68), cells were fixed and permeabilized using a combination of paraformaldehyde and saponin as part of the BD Biosciences fixation/permeabilization kit (BD Biosciences). Cells were retrieved from the fibrin gel by digestion with either 2.5% Trypsin or 50 FU/ml Nattokinase [29] (Japan Bioscience Ltd). Fluorescently activated cell sorting (FACs) was used to sort monocytes into CCR2+/−, or CD16+/- populations, using a BD FACs Diva sorter. We used the corresponding isotype control antibodies in the same quantities to choose the appropriate gates for sorting (Fig. S3).

2.7. Trans-well migration assay

A confluent monolayer of endothelial cells was formed on the trans-well membrane with pore size of 8 μm. 150×10^3 HUVECs were placed on the membrane, 2 days prior to adding the monocytes on top of the monolayer to attain confluence. Inflammatory monocytes were placed on top of the confluent monolayer, 10 nM chemokine ligand 2 (CCL2) was added to the media in the well below the trans-well to induce their migration. In a different set of experiments, inflammatory monocytes were placed on top of trans-well membranes with a pore size of 3 or 8 μm 10 nM of CCL2 was added to the media in the bottom well to induce migration of monocytes through the trans-well membranes. Two hours later, the monocytes that migrated through the membrane were retrieved from the bottom of the well with a cell scraper. To count the number of monocytes that migrated through the trans-well membrane, we added a fixed number of fluorescent cell counting beads (ThermoFisher, CountBright Absolute Beads) to each sample before running it through the flow cytometer, so that the ratio of sample volume to microsphere volume was known. The flow cytometer was used to count the number of cells and beads in part of the sample. Knowing the original number of beads added to the sample (typically 10 000), allows us to back calculate the original total number of cells in the sample. The monocyte extravasation rate was approximated by the bead count as the number of monocytes retrieved from the well divided by the total number of monocytes originally seeded on top of the trans-well.

2.8. Immunostaining

Immunostaining was performed to detect CD206 positive cells. Devices were fixed with 4% paraformaldehyde for 10 min, permeabilized with 0.1% Triton X, and blocked with a blocking buffer containing FcR blocking reagent to minimize unspecific binding. The primary antibody was also incubated with FcR Blocking overnight at 4 °C, washed and counterstained with a AlexaFluor 568 nm secondary antibody for 4 h. Devices were washed and imaged within 2 days. We validated the specificity of the antibody signal by simultaneously imaging a separate sample stained with the isotype control.

2.9. Image analysis

Time-lapse and single confocal images were analyzed using 3D segmentation software (Imaris). Typically, the microvascular network, monocytes and fibroblasts were semi-automatically segmented into 3D surfaces; all resulting surfaces were manually checked and modified if necessary (Fig S1C). Monocytes were manually detected with respect to their location (i.e. intra- or extravascular), by looking at the cross-section of the vessels (Fig. S1B). A monocyte was defined as extravasated if its entire body was found in the 3D fibrin gel around the microvascular network. The distance transformation function provided by Imaris XT was used to compute the minimum distance from each cell centroid to the microvascular network. For time-lapse images, the microvascular network's centroid was used as a reference point to account for any drift, since only minimal change in the network morphology was observed within 10 han. A custom-written Matlab code was used to compute cell speed and displacement using the x,y,z coordinates of all segmented surfaces provided by Imaris.

2.10. Statistical analysis

Statistics were performed using Matlab. To test for statistical significance between independent groups of variables, an unpaired t-test is used. Students' t-tests were used between 2 independent variables, and ANOVA for more than one variable, with the threshold of significance for the p-value chosen as 0.05, unless otherwise noted. To test whether a change in a variable was significant, we used a one-sample student's t-test to test the hypothesis that the mean change was significantly different from 1. Unless specified otherwise, data is reported as the average ± SEM.

3. Results

3.1. Monocytes transmigrate through the microvascular networks and interact with fibroblasts

Human fibroblasts and endothelial cells were seeded into the microfluidic device successfully yielding perfusable microvascular networks within 5 days, as we [26] and others [30] previously described. Briefly, endothelial cells elongated and migrated within the 3D fibrin gel over time, forming a network of 3D interconnected vessels. Fibroblasts have been shown to be important for inducing vessel lumen formation [30]. Fibroblasts were found to closely associate with the endothelial vessels, within 10 μm of the vessel wall ($p = 1.1 \times 10^{-5}$, one-way ANOVA; Fig. S2A). Vessel height was measured to be 6.4 ± 0.7 μm. The variance in cross-sectional area was much higher than vessel height, as the microvascular network consisted of branches of varied sizes averaging 1190 ± 307 μm^2 (Fig S1D).

Within 1 h following monocyte perfusion into the networks, most monocytes (62 ± 5%) were trapped in vessel lumen while the rest were adhered to the vessel wall. Extravasation of monocytes did not occur immediately following perfusion, as noted by the lack of extravasation events within 2 h following perfusion. At 8 h post-perfusion, 9.7 ± 5.4% of the monocytes were found outside of the vessels, which increased to 59.2 ± 8% at 24 h and 79 ± 10.4% at 48 h (Fig. 1B). A high variability existed between donors: the coefficient of variation of extravasation rate at 24 h between donors was 30.3 ± 7.5%. The actual process of extravasation occurred very rapidly once initiated. The bulk of the cell body typically crossed the endothelial wall in less than 3 min (Fig. 1C), making these events extremely difficult to capture. Fig. 1 (Fig. 1C and Supplemental Movie 1) highlights such an event. During extravasation, monocytes extend protrusions through the endothelial wall into the surrounding fibrin gel, while the bulk of their body remains spherical and inside the vessel (Fig. 1C). After extravasation, monocytes inhabited the extravascular space (Fig. 1D/E). Monocytes were never observed to re-enter a vessel.

Analyzing the co-localization of fibroblasts and endothelial cells (Supplemental Fig. 2C), demonstrates that, on average, 27.1 ± 5.2% of the endothelium was in direct contact with fibroblasts. Prior studies suggest that fibroblasts may regulate transmigration of monocytes [31], therefore we examined this directly by modulating the concentration of fibroblasts. No correlation between fibroblast concentration and monocyte extravasation efficiency exists within the range of fibroblasts densities tested (Supplemental Fig. 2B). Also, extravasation rate of monocytes remained unchanged in regions with less coverage of the endothelium by fibroblasts (data not shown). Following their extravasation, 29 ± 5% of monocytes appeared to be in direct contact with fibroblasts within the extra-luminal space.

3.2. Inflammatory CCR2+, but not patrolling CCR2-, monocytes extravasate in our assay, mimicking in vivo behavior.

In vivo studies have shown that inflammatory monocytes are more prone to extravasate than patrolling monocytes [32]. We show, using our *in vitro* assay, that we can replicate this extravasation pattern. Using FACs, we first sorted whole monocyte populations into subgroups depending on CD14 and CD16 expression. The inflammatory (CD14$^+$CD16$^-$) population of monocytes was found to be significantly larger than that of patrolling (CD14$^-$CD16$^+$) and intermediate (CD14$^+$CD16$^+$) monocytes (Fig. 2A; $p = 3.6 \times 10^{-16}$, 1-way ANOVA). The ratio of the different subpopulations of monocytes was remarkably consistent across donors: 69.3 ± 2.8% of monocytes were inflammatory, 15.5 ± 3.1% patrolling, and 9.7 ± 1.9% intermediate monocyte populations. It is also known that patrolling monocytes do not express CCR2, while inflammatory and intermediate monocytes do [5]. Our results confirm that CCR2+ and inflammatory monocyte subpopulations largely overlap (Fig. 2B): the majority of CCR2+ monocytes are also CD16$^-$and CD14$^+$, while the majority of CCR2-were CD14$^-$and CD16$^+$. There remains a smaller number of CCR2+ monocytes that are CD14$^+$ and CD16$^+$, most likely corresponding to the intermediate subpopulation of monocytes (CD14$^+$CD16$^+$). Next, we investigated whether inflammatory or patrolling monocytes have different extravasation capacity in our system. We also looked at whether the presence of CCR2 in monocytes is a predictor of their extravasation capacities. We introduced each subpopulation into separate microvascular networks and demonstrated that inflammatory monocytes have a much higher tendency to extravasate than patrolling monocytes ($p = 0.006$), consistent with *in vivo* observations. After 1–4 days, 84 ± 7% of inflammatory monocytes had transmigrated, in contrast to 12 ± 10% of the patrolling monocytes

(Fig. 2C). Similarly, we sorted monocytes into CCR2 positive and negative populations, and observed a clear and statistically significant distinction in their transmigration efficiencies: after 2 days, 91 ± 4% of CCR2+ monocytes were extravascular, versus 13 ± 4% for CCR2-monocytes (Fig. 2C/2D).

In order to further characterize the differences in phenotype between inflammatory and patrolling monocytes in our assay, we quantified their intravascular displacement and speed. Using time-lapse confocal microscopy, we found that patrolling monocytes had a much lower intravascular net displacement (21.1 ± 3.1 versus 45.1 ± 6.3 µm, respectively; $p = 3.1 \times 10^{-8}$,Fig. 2E) and speed (1.80 ± 0.012 vs. 0.83 ± 0.07 µm/min; $p = 2.6 \times 10^{-10}$ (Fig. 2F) compared to inflammatory monocytes (Supplementary Video 2). For the few patrolling monocytes that did extravasate, there was no significant difference in their speed after transmigration: 0.70 ± 0.06 vs 0.49 ± 0.14 µm/min ($p = 0.20$). Overall, these results indicate that the monocytes that extravasate in our assay are of inflammatory origin and CCR2+ phenotype, as observed *in vivo*. These findings demonstrate our assay as a physiologically relevant model for investigation of monocyte extravasation.

Supplementary video related to this article can be found at https://doi.org/10.1016/j.biomaterials.2018.03.005

3.3. Inflammatory monocytes depend more largely on actomyosin-based motility than patrolling monocytes

Based on our observations of large differences in speed between patrolling and inflammatory monocytes, we hypothesized that these subpopulations might use different motility mechanisms. Cells typically rely on actomyosin contractility for movement to varying extents. Research suggests that myosin IIA is important in T-cell or neutrophil motility and extravasation [33], but no evidence exists in relation to monocytes. We therefore investigated the role of actomyosin on motility in different monocyte subsets using the reversible myosin IIA-inhibitor blebbistatin. First, we show that both patrolling and inflammatory monocytes express myosin IIA (Fig. 3A). We then exposed both inflammatory and patrolling monocytes to 50 µM blebbistatin (or DMSO) for 20–30 min while in suspension, which has been shown to block myosin II in monocytes and macrophages in other studies [34,35]. First, we show that blebbistatin changes the phenotype of inflammatory monocytes in 2D [34]; we observed that inflammatory monocytes pre-treated with blebbistatin have a larger area of adhesion, as previously reported for T cells treated with blebbistatin [36] (Fig. 3B). We examined the effects of blebbistatin on intravascular migration for both monocyte subpopulations. Our results demonstrate that blebbistatin significantly slows inflammatory monocyte migration along the microvascular wall, but not that of patrolling monocytes (Fig. 3C). On average, blebbistatin significantly lowers the migration rate of inflammatory monocytes by 45.5 ± 1.8% ($p = 0.002$). For blebbistatin or DMSO pre-treated inflammatory monocytes, speed was 2.16 ± 0.50 versus 4.00 ± 0.98 µm/min, respectively. In contrast, patrolling monocyte speed remained unchanged ($p = 0.6$, 0.80 ± 0.15 vs. 0.67 ± 0.06 µm/min for treated and control, respectively). For blebbistatin or DMSO pre-treated patrolling monocytes, speed was 0.80 ± 0.15 vs. 0.67 ± 0.06 µm/min, respectively. Note that there were many less patrolling monocytes to analyze, since they were found in less quantity in the blood (Fig. 2A). In addition, we tested whether actomyosin contractility plays a role in inflammatory monocyte extravasation, which has been shown to be the case for neutrophils, where myosin IIA facilitates nuclear squeezing during neutrophil transmigration [33]. Despite pre-treatment with blebbistatin, no significant differences in extravasation efficiency of inflammatory monocytes was observed through the microvascular networks, 8 h after exposure to the drug (Fig. 3D). We repeated the
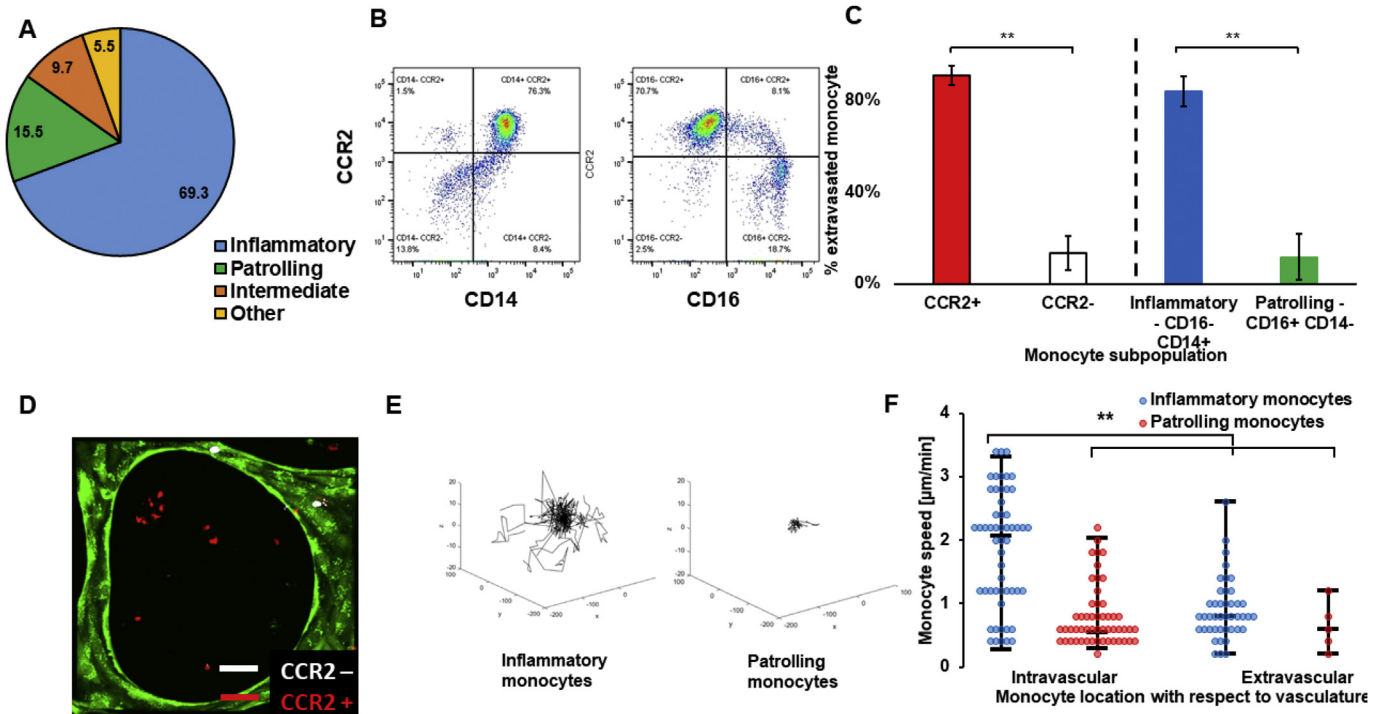
Fig. 2. **Inflammatory CCR2+ monocytes but not patrolling or CCR2-monocytes extravasate in our assay, mimicking *in vivo* behavior**. A) Pie chart showing the average percentage of the different monocyte subpopulations in blood samples from N = 7 donors. B) Representative flow cytometry plot, showing the percentage of CCR2+ or − monocytes that are either CD16+/− or CD14+/−, showing there is a large overlap between CCR2+ monocytes and inflammatory monocytes (CD14$^+$CD16$^-$) and between CCR2-and patrolling monocytes (CD14$^-$ CD16$^+$). C) Percentage of subpopulation of monocytes found in the extravascular space 2–3 days following monocytes perfusion inside the microvascular network. In one set of experiments, monocytes were sorted into inflammatory (CD14$^+$CD16$^-$, blue) or patrolling (CD14$^-$ CD16$^+$, green) monocytes, while in another set of experiments, monocytes were sorted into CCR2 positive (CCR2+, red) or CCR2 negative (CCR2, white). N = 3 devices, N = 3 donors. Bars are SEM. D) Confocal projection image of CCR2+ and CCR2-monocytes perfused together in a microvascular network. CCR2-monocytes (white) were typically found inside the vessels, while CCR2+ (red) had a much higher tendency to extravasate and be found in the extravascular space. E) Representative trajectories of either inflammatory or patrolling monocytes during their intravascular migration. F) Speed of inflammatory (blue) vs. patrolling (red) monocytes found intravascularly or extravascularly one day following perfusion in the microvascular networks. Each point corresponds to one monocyte. N = 47–61 cells, N = 3 devices, N = 3 donors.

experiment on an endothelial monolayer in a trans-well. This confirmed that blebbistatin did not affect monocyte trans-endothelial migration within 2 h of exposure to the drug (Fig. 3E). In addition, blebbistatin did not decrease monocyte migration through 8 or 3 μm pores, confirming that myosin IIA is not the key facilitator of monocyte transmigration (Fig. S4). Moreover, monocytes also depend on actomyosin contractility following their trans-endothelial migration. We demonstrate this by adding 50 μM of blebbistatin in the microfluidic device for 1–2 h 2 days after introducing the monocytes, when most have extravasated. Blebbistatin caused a decrease in extravascular monocyte speed of 43.4 ± 10% (p = 0.055; Fig. 3F). In blebbistatin or DMSO treated samples, monocyte speed was 0.87 ± 0.10 vs. 0.45 ± 0.04 μm/min, respectively. Combined, our results suggest that different monocyte's subsets employ distinct mechanisms of motility, and that monocytes might not use similar mechanisms for extravasation as other immune cells.

3.4. After extravasation, monocytes slow down, stay perivascular and become macrophage-like

Following extravasation, most monocytes stayed within 10–20 μm of the vessel wall (p = 0.0014; one-way ANOVA; Fig. 4A), with 58 ± 5.0% of them found within 10 μm. One day after monocyte perfusion, 25.2 ± 11.6% of extravascular monocytes were in direct contact with the endothelium. Monocytes significantly changed shape after extravasation, which is a strong indicator of

their change towards a macrophage-like phenotype. Monocytes in the intravascular space remain spherical, while those that extravasated exhibit more protrusions and a decrease in their sphericity that was accentuated over time (Fig. 4B; 0.93+-0.01 for intravascular versus 0.80+-0.01 for extravasated cells at day 3, p = 0.002). Two days after extravasation, monocytes movement drastically decreased (mean displacement of 0.17 ± 0.01 μm/min) despite the observation of many cellular protrusions. We found no significant correlation between monocyte speed and distance from the endothelium (Fig. S5A). We did not see any obvious breach in laminin or collagen IV following monocyte trans-endothelial migration (Fig. S5B/C).

Immunostaining confirmed that most of the monocytes around the microvascular networks highly expressed the maturation marker CD206 (Fig. 4C), indicating that monocytes upregulated macrophage-like markers. There was no correlation between proximity to the vessel and CD206 expression (data not shown). We further characterized monocyte differentiation by analyzing the expression of more macrophage-like markers, CD206, CD68 and CD163 using flow cytometry. In addition, we tested whether macrophage differentiation was directly linked to the process of extravasation itself. Freshly isolated monocytes were separated into 3 samples. The first sample was immediately analyzed while still in suspension (Fig. 4D). The second sample was perfused in the macro-vascular networks and allowed to extravasate over time. The third sample was placed in a fibrin gel with the endothelial cells and fibroblasts. This latter assay did not give monocytes an
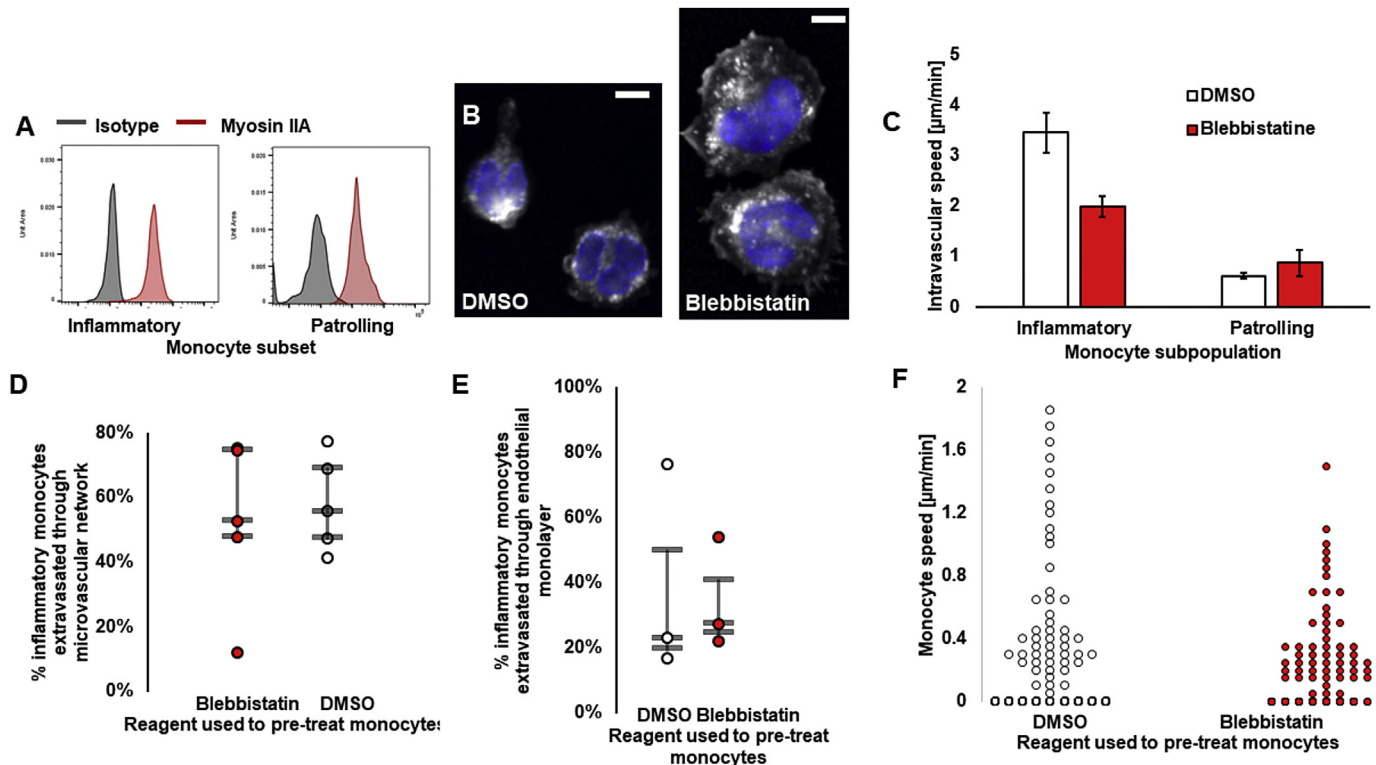
Fig. 3. Inflammatory monocytes depend more largely on actomyosin-based motility than patrolling monocytes. A) Myosin IIA expression of inflammatory and patrolling monocytes. B) Microscopy images of inflammatory monocytes in 2D pre-treated with DMSO or blebbistatin, fixed within 30 min of exposure to the drug. Nucleus is shown in blue. Cytoplasm is shown in white, stained with Cell Tracker. Bars are 5 μm. C) Intravascular monocyte speed, of either inflammatory or patrolling monocytes treated with Blebbistatin (red) or DMSO (white). Bars are SEM. D) Extravasation rate of inflammatory monocytes treated with Blebbistatin (red) or DMSO (white) 8 h after delivery into the microvascular networks and exposure to the drug. Each circle represents the result from a microfluidic device. E) Extravasation rate of inflammatory monocytes treated with Blebbistatin (red) or DMSO(white) through a confluent endothelial monolayer formed on top of a trans-well membrane with 8 μm pores. Each circle represents the result from one trans-well. For D and E, the bars represent the third quartile, the median and first quartile of population. F) Speed of extravascular monocytes, treated with Blebbistatin (red) or DMSO (white) 2 days after their delivery in the microvascular networks. Each circle represents one monocyte (N = 2 Donors, N = 3 devices per condition, N = 60—64 cells). (For interpretation of the references to colour in this figure legend, the reader is referred to the Web version of this article.)

opportunity to extravasate since no vessels were formed to start with, but still exposed the monocytes to the same signaling factors produced by endothelial cells and fibroblasts. After four days (selected to maximize the number of extravasated monocytes, 63.2 ± 9.7% in this case), monocytes were retrieved from both assays and analyzed by flow cytometry (Fig. 4E). In both conditions, monocytes clearly upregulate CD206, CD163 and CD68 expression, markers of macrophage differentiation. This suggests that, in our assay, extravasation is not essential for monocyte differentiation.

3.5. Variability in tumor cell extravasation is not solely explained by local microvascular network characteristics

Our microfluidic platform is primed for studies involving cancer cell extravasation, as we have previously shown [37]. Here, we observed that, similar to our observations for monocyte extravasation, fibroblasts do not affect cancer cell extravasation (data not shown), and cancer cells significantly change shape after they extravasate (Fig. 5A). We also observed that 62.8 ± 23.8% of tumor cells were physically trapped in the micro-vessels following their transient perfusion through the microvascular networks. We show that there is no difference in the intravascular migration between the cancer cells that eventually extravasate and those that do not. Tumor cells that eventually extravasate do not seem to move faster, or to explore a larger volume of the vasculature (Fig. 5B/5C) This suggested that intravascular migration does not dictate extravasation efficiency of cancer cells in our assay. We proceeded to test

whether extravasation rate depends instead on their specific location within the microvascular network. First, we see that there is in fact a high variability in the extravasation efficiency between groups of tumor cells that are found in separate regions of the networks. The coefficient of variation in extravasation rates of tumor cell groups between experiments was 125 ± 10.5%. This suggested that tumor cell extravasation might be dictated by local variations in the microvascular networks. To test this, we examined differences in tumor cell confinement. Our results show, physically trapped tumor cells did not have a higher tendency to extravasate than adhered tumor cells (Fig. 5D). Although we speculated that extravasation could be affected by local variations in the microvascular network other than its size, tumor cells in close proximity did not behave similarly (Fig. 5E/F). Therefore, our data suggests that tumor cell extravasation cannot solely be explained by local changes in the endothelium.

3.6. Tumor cell extravasation is affected by monocytes

Whether monocytes directly engage with tumor cells inside the vasculature and affect tumor cell extravasation remains to be seen. Here, we employ two experiments to determine the influence of monocytes on tumor cell extravasation (Fig. 6A/D). Each experiment mimics monocytes at different stages of their differentiation. In the first one, tumor cells and undifferentiated monocytes are perfused together in the vasculature, mimicking their interaction in the bloodstream. We show that intravascular monocytes reduce the
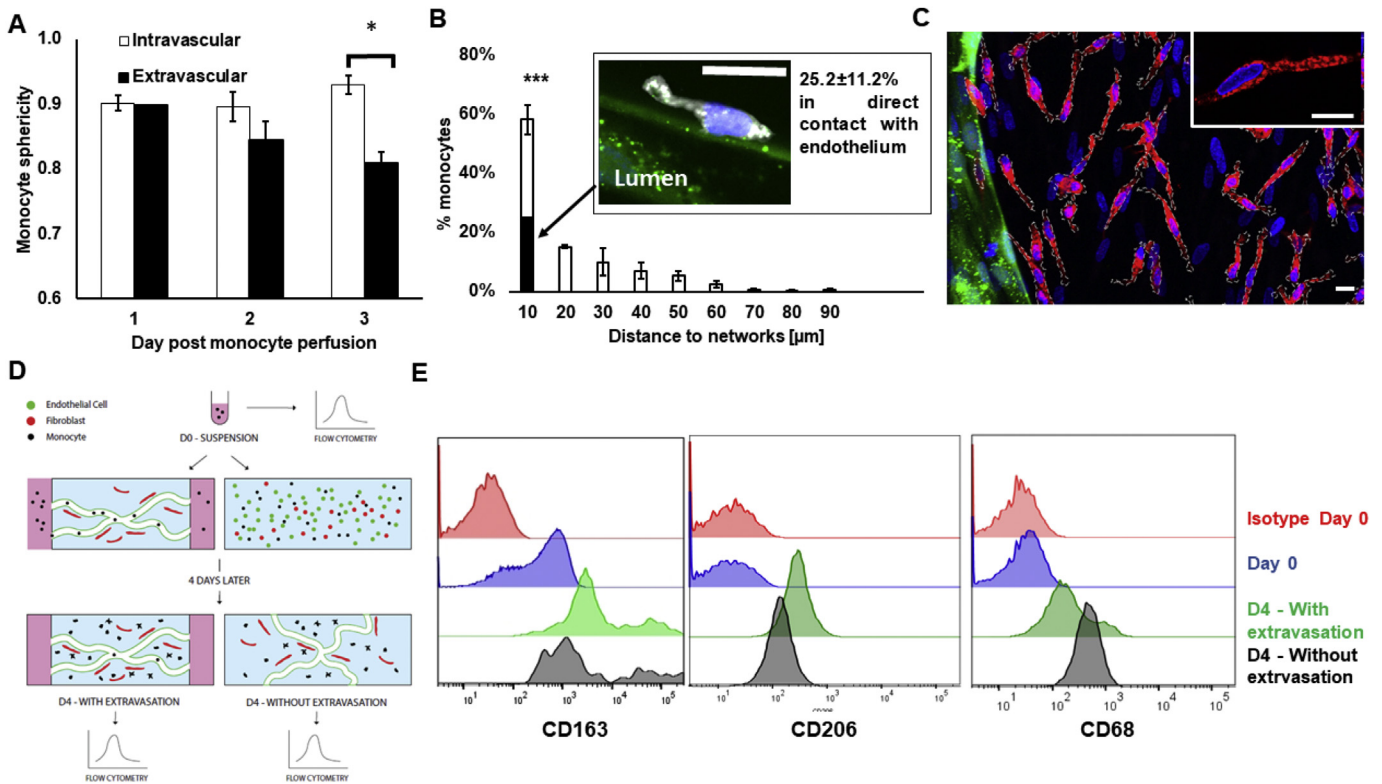
Fig. 4. After extravasation, monocytes slow down, stay perivascular and become macrophage-like. A) Sphericity of intravascular vs. extravascular monocytes over time following their perfusion in the microvascular networks. B) Histogram showing the distribution of monocyte with respect to their minimum distance to the endothelium wall. The filled portion of the bar shows the percentage of monocytes that are in direct contact with endothelium. N = 3–8 devices, N = 3 donors. The confocal microscopy image shows a perivascular monocyte (white) following its extravasation (nucleus stained with DAPI in blue) in direct contact with endothelium (green). N = 3–8 devices, N = 3 donors. Bar is 10 μm. C) Representative confocal image showing monocytes after transmigrating through vascular network (green) stained with CD206 (red). Nuclei are shown in blue (DAPI). Monocytes membranes are surrounded by white dashes. Note that there are also fibroblasts in the extravascular space, which correspond to the nuclei that are not part of a cell overlaid with white dashes. Bars are 10 μm. D) Diagram describing experiment to characterize monocyte differentiation status over time. Macrophage-like markers CD68, CD163 and CD206 were analyzed with flow cytometry on monocytes at different time points: immediately after blood isolation; or four days later, after the monocytes were either introduced in the vascular networks, allowed to extravasate, and retrieved for analysis or mixed with endothelial cells and fibroblasts in a 3D fibrin gel to expose them to the same micro-environment factors but without giving the monocytes a chance to extravasate. E) Representative flow cytometry tracings corresponding to experiment just described for CD68, CD163 and CD206.

rate of tumor cell extravasation (Fig. 6C). Within 10 h, there is a 42% reduction in MDA-MB-231 extravasation. In the second set of experiments, monocytes were first introduced in the vascular networks alone, followed by the tumor cells a few days later (once most monocytes had entered the extravascular space and become macrophage-like). In this way, we mimic the interactions between tissue monocyte-derived macrophages and tumor cells that had just stopped at the secondary site. In the latter case, no significant effect on tumor cell extravasation was seen in the presence of monocyte-derived macrophage over the course of 4 days ($p > 0.4$; Fig. 6F). However, MDA-MB-435 were affected more on day 3 ($p = 0.06$). Proliferation, as evidenced by the formation of small tumor cell clusters, was not enhanced by macrophages (data not shown). Of note, while we did rarely observe phagocytosis of fibroblasts or vascular material by monocytes, we never observed tumor cells being phagocytosed directly by monocytes, neither did we observe during the time-lapse images any evidence of monocyte-induced tumor cell apoptosis.

In order to investigate how monocytes reduced tumor cell extravasation, we looked at whether monocytes affected cancer cell extravasation by altering the endothelial barrier. Our results show, that within 48 h, permeability of the endothelium remained unchanged in the presence of monocytes Fig. 7A/B). This begs the question as to whether the effect is purely due to steric hindrance. In our system, tumor cells that extravasated were as likely to be in

contact with monocytes than tumor cells that did not extravasate (Fig. 7C/D). This suggests that direct contact between monocytes and cancer cells does not alone explain the reduction in tumor cell extravasation. Similarly, we do not see a trend suggesting that tumor cells that had prolonged contact with monocytes moved at a different speed inside the vessels (Fig. 7E). Finally, no difference in intravascular speed, or in the volume travelled (data not shown) was observed between tumor cells in assays where they were perfused alone or with monocytes (Fig. 7F). These results demonstrate that monocytes did not reduce tumor cell extravasation by affecting the tumor cell migratory behavior inside the vessels; rather, we speculate that monocyte-associated paracrine signaling was the cause of decreased tumor-cell extravasation. We performed a cytokine array (RayBiotech, Array C5) to screen for cytokines and chemokines produced by monocytes. Note that the media used in this array was conditioned by monocytes cultured in 2D, and not in the microfluidic device. Mainly, this was meant to maximize the concentration and volume of conditioned media; that is, media collected from a microfluidic device would not surpass 400 μL in this study. Future studies should however further examine media conditioned by cells in three-dimensions as these it might differ. Our qualitative results suggest that monocytes produce an important amount of CCL24, CCL2, CXCL7, GRO $_{a/b/g}$, IL-8, TIMP-1, TIMP-2 and some CCL5 many of which have been associated to different cancers [18,38–41]. Our findings suggest that monocyte-tumor cell
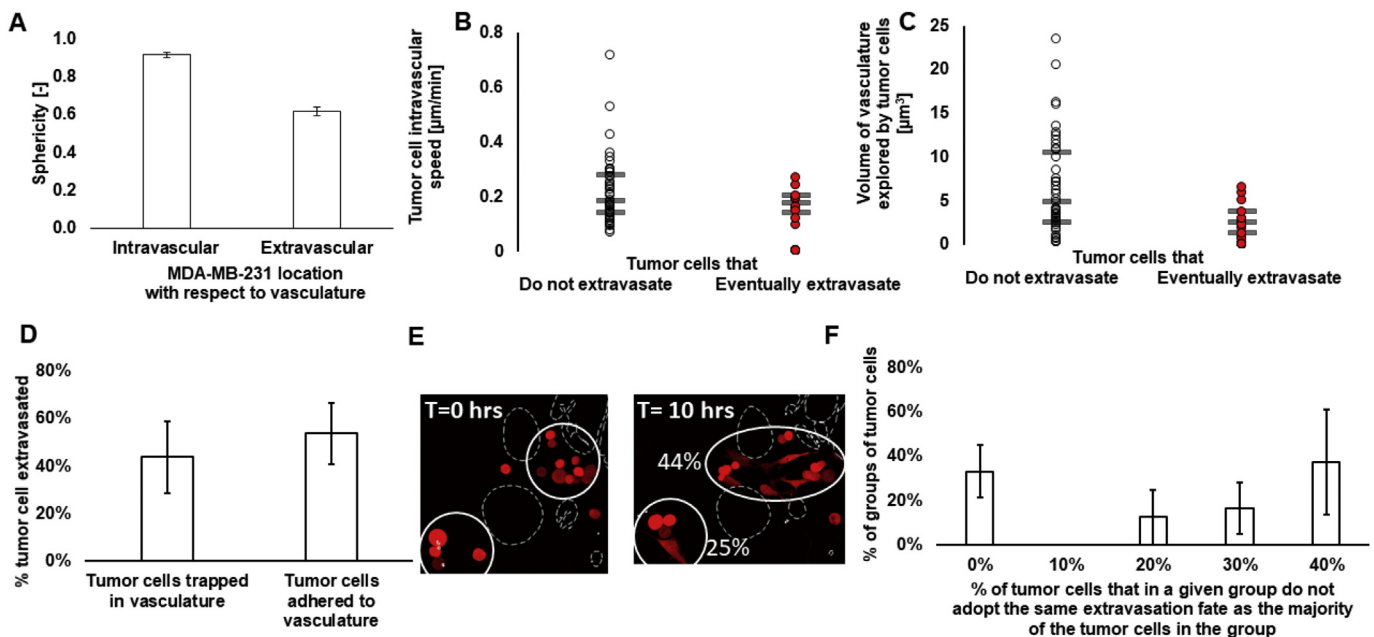
Fig. 5. Variability in tumor cell extravasation is not solely explained by local microvascular network characteristics. A) Sphericity of tumor cells (MDA-MB-231) before or after they transmigrate through the microvascular network. N = 4 experiments, N = 4 donors. B) Intravascular speed of tumor cells (MDA-MB-231) that do not extravasate (white circle) or that do eventually extravasate (red circle) during the time-lapse. Each circle represents a tumor cell. N = 3 experiments, N = 40—44 cells. C) Volume of the vascular networks explored by the tumor cells (MDA-MB-231) that do not extravasate (white circle) or that do eventually extravasate (red circle) during the time-lapse. Each circle represents a tumor cell. N = 3 experiments, N = 40—44 cells. For C&D, the bars represent the third quartile, the median and first quartile of population. D) Representative confocal image of groups of tumor cells (red) in different regions that extravasate at different rates in a segment of a microvascular network (shown by dashed white line). The second image shows the same tumor cells 10 h later, with the extravasation rate of the group of tumor cells comprised in the white circle. Bar is 20 μm. E) Percentage of tumor cells (MDA-MB-231) that extravasated grouped as a function of whether they were originally trapped in the microvascular network or adhered to the endothelium. Bars are SEM. F) Histogram showing the percentage of tumor cells in a given group of cells that do not adopt the same extravasation fate as the majority of the group. We see that tumor cells in the same region are not likely to always extravasate or to always stay intravascular. N = 4 experiments, N = 15 groups of tumor cells composed of 2—10 cells. Bars are SEM. (For interpretation of the references to colour in this figure legend, the reader is referred to the Web version of this article.)

signaling warrants further examination, and have therapeutic potential in reducing metastatic progression.

4. Discussion

We characterize a novel application of a 3D vascularized microfluidic model to study monocyte physiology as they transmigrate through human microvessels. We demonstrate the first high-resolution time-lapse image of a monocyte as it extravasates through a 3D human *in vitro* vessel (Fig. 1C & Supplementary Video 1). We demonstrate our model is physiologically relevant by detecting differences in the transmigration of distinct monocyte subsets that have been previously reported *in vivo*. We demonstrate differences in myosin IIA dependence between monocyte subpopulations. In our assay, monocytes found in the extravascular space became macrophage-like but had no effect on the ability of cancer cells to extravasate through the vasculature. In contrast, undifferentiated monocytes present with cancer cells in the intraluminal vasculature reduced MDA-MB-231 extravasation. Furthermore, high-resolution time-lapse imaging revealed that monocytes did not limit cancer cell extravasation rate in a purely contact-dependent fashion. Further research is necessary to uncover the mechanisms underlying the anti-metastatic effects of monocytes observed in this study, which could represent a promising therapeutic avenue to slow down cancer progression.

While intravital imaging has unveiled crucial information about monocyte movement both intravascularly [42], or extravascularly as monocyte-derived macrophages [43], it has proved much harder to visualize their trans-endothelial migration in mice. *In vitro* studies of monocyte extravasation typically consist in trans-well or collagen gel migration assays. While useful to screen for surface receptors involved in locomotion and transmigration [44,45], the planar monolayers do not recapitulate the geometry of vessels. In our system, we demonstrate monocyte entrapment in physiologically relevant human micro-vessels. Endothelial permeability, as measured in our 3D system (10^{-7} cm/s), is similar to *in vivo* magnitudes [46]. Our images show the bulk of the cell body crossing the vessel in less than 3 min. This is consistent with the short time (~0.8 min) taken by neutrophils to cross endothelial monolayers [33] as well as monocytes [44] *in vitro*.

Similar to *in vivo* studies, we show heterogeneity in extravasation efficiency between monocyte's subsets (Fig. 2C/D). We show that inflammatory monocytes extravasate much more frequently than patrolling monocytes, as observed *in vivo*. Studies have shown that monocytes' locomotion, as well as their surface receptors and their binding to endothelial adhesion molecules play a key role in their extravasation [44,45]. In parallel, it is known that patrolling and inflammatory monocytes have different migration modes [47], and express different surface receptors [48]. Therefore, the differential extravasation potential of these distinct monocytes subsets could be largely explained by their different surface receptors, migratory properties and differential affinities to endothelial cell's surface receptors. We report a speed of inflammatory monocytes that is similar to that observed on a monolayer under shear (~2 μm/min [47]), which agrees with results observed *in vivo* [49]. *In vivo*, inflammatory monocytes are recruited from the bone marrow in a CCL2-dependent manner [50], a chemokine that was heavily produced both by HUVEC and fibroblasts in our assays (ELISA, data not shown). Little is known about the extravasation abilities of patrolling monocytes, except that this is rarely observed in
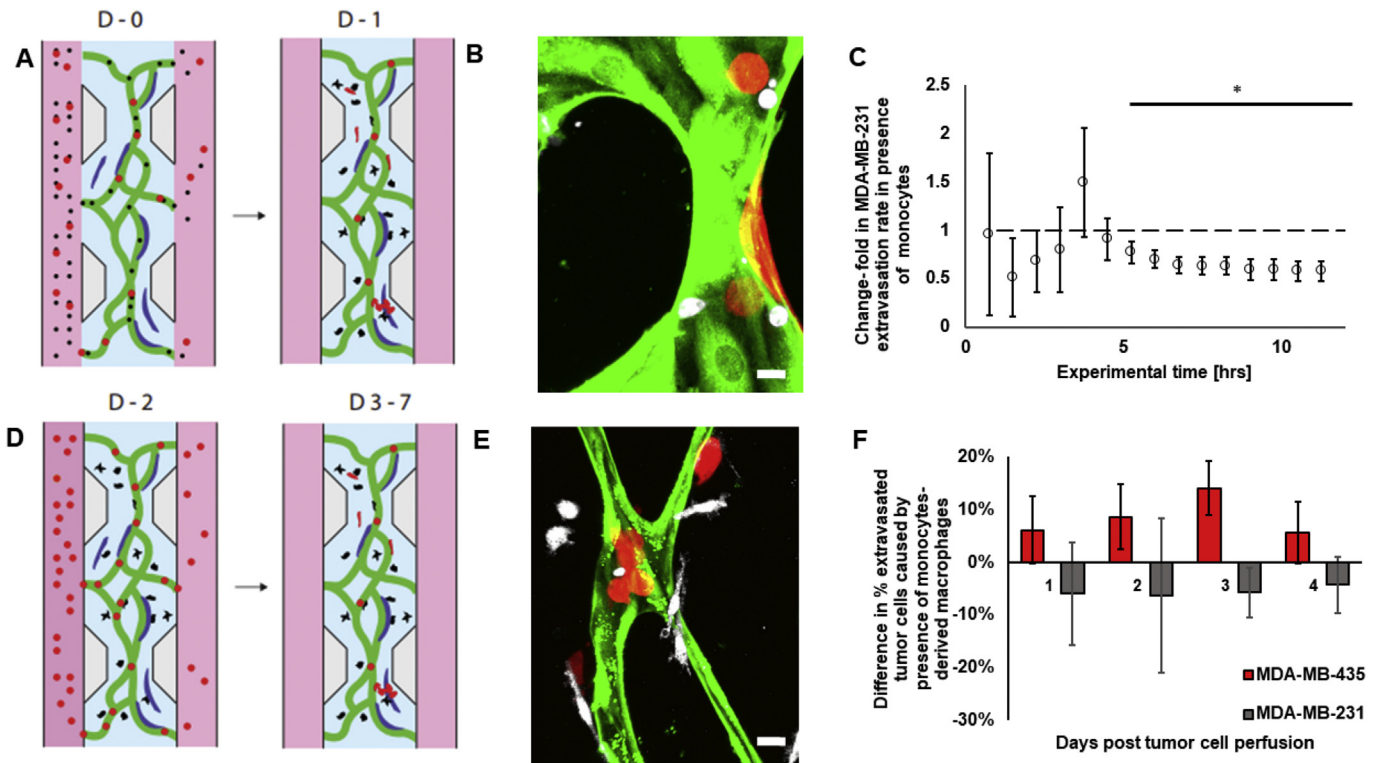
Fig. 6. Tumor cell extravasation is affected by monocytes before the monocytes transmigrate through the vessels. A) Diagram of the experiments performed with monocytes (black) perfused in the microvascular network (green) directly with the tumor cells (red). In this diagram, fibroblasts are shown in blue. B) Corresponding confocal image. Monocytes are in white, tumor cells in red, endothelial cells in green; fibroblasts not visible. Bar is 10 μm. C) Change in extravasation rate of MDA-MB-231 tumor cells caused by the presence of monocytes. Bars are SEM. D) Diagram of the experiments performed with monocytes (black) after they transmigrated through the microvascular networks. In these experiments, monocytes were first perfused on their own in the microvascular networks as previously described (Fig. 1A) − two days later, most of them had crossed the endothelium, at which point the tumor cells were perfused in the microvascular networks. In this diagram, fibroblasts are shown in blue. E) Corresponding confocal image. Monocytes are in white, tumor cells in red, endothelial cells in green; fibroblasts not visible. Bar is 10 μm. F) Quantification of the change in tumor cell extravasation (MDA-MB-231 in grey, and MDA-MB-435 in red, separate experiments) caused by the presence of monocyte-derived macrophage. For MDA-MB-435, 167−343 cells in 7−12 devices were analyzed per condition per day. For MDA-MB-231, 77−285 cells in 2−6 devices per condition were analyzed per day. Bars are SEM.

homeostatic conditions [51], which agrees with the minimal extravasation efficiency observed in our assay Interestingly, it has been shown that they can extravasate in the peritoneum of mice following bacterial infection [42]. We see that patrolling monocytes move at 0.70 ± 0.06 μm/min (Fig. 2F) which is significantly lower than that reported *in vivo* (~10 μm/min) [1]. We suspect the absence of flow, or lack of key adhesion molecules on HUVECs, might contribute to this difference. In particular, CX_3CL_1 has been shown to be important for the arrest of patrolling monocytes at inflammatory sites [51], but was not detected in our system (ELISA, data not shown). Indeed, higher speeds, similar to those reported *in vivo*, have been observed for patrolling monocytes on an endothelial monolayer under shear flow. In fact, blocking CX_3CL_1 in that study was shown to eliminate the long range motility of patrolling monocytes [47], thus supporting the idea that its absence in our assay might explain the stagnation of patrolling monocytes.

Myosin IIA has been shown to be important for neutrophil [33] and T cell [52] motility and extravasation. Studies have investigated the role of myosin IIA only in monocytes readily differentiated into macrophages [35], non-human macrophages [53], or monocytes that were not separated into its functionally distinct subsets [54]. This is the first study that dissects the role of myosin IIA in monocyte motility as it progresses from the intravascular space, transmigrates through the endothelium and migrates through the extravascular compartment. Intravascular migration of inflammatory but not patrolling monocytes was partially blocked by myosin

IIA inhibition (Fig. 3C). This suggests that patrolling monocytes rely on other mechanisms for movement − for example, on actin polymerization for short-range motion. This difference in acto-myosin dependence between monocytes' subsets might reflect their different functions, and different modes of migration previously reported in the literature [47]. Note that these might also change under different conditions: it would be interesting to test whether under inflammatory conditions, patrolling monocytes switch to an acto-myosin-based motility, to perform certain tasks. Our results show that myosin IIA might not be required for monocyte trans-endothelial migration (Fig. 3D/E). This differs from studies performed on T cells [52] or neutrophils [33] which showed reduced extravasation through an *in vitro* endothelial monolayer upon exposure to blebbistatin. Reduced immunocyte infiltration to the kidneys in a rat with obstructive nephropathy [53] has also been observed following myosin IIA inhibition. This could suggest monocytes employ different mechanisms to extravasate, or perhaps monocytes do depend on myosin IIA when activated by inflammation, which was not the case in our experiments. Finally, blebbistatin also had a significant effect on extravasated monocyte speed (Fig. 3F), which agrees with studies demonstrating significant slowing of blood-derived monocytes in 2D and 3D collagen matrices [54]. Of interest, myosin II plays a fundamentally different role in suspended versus adherent cells, as shown by a study that used blebbistatin and observed increased stiffness of monocytes in suspension, but no effect after their differentiation into
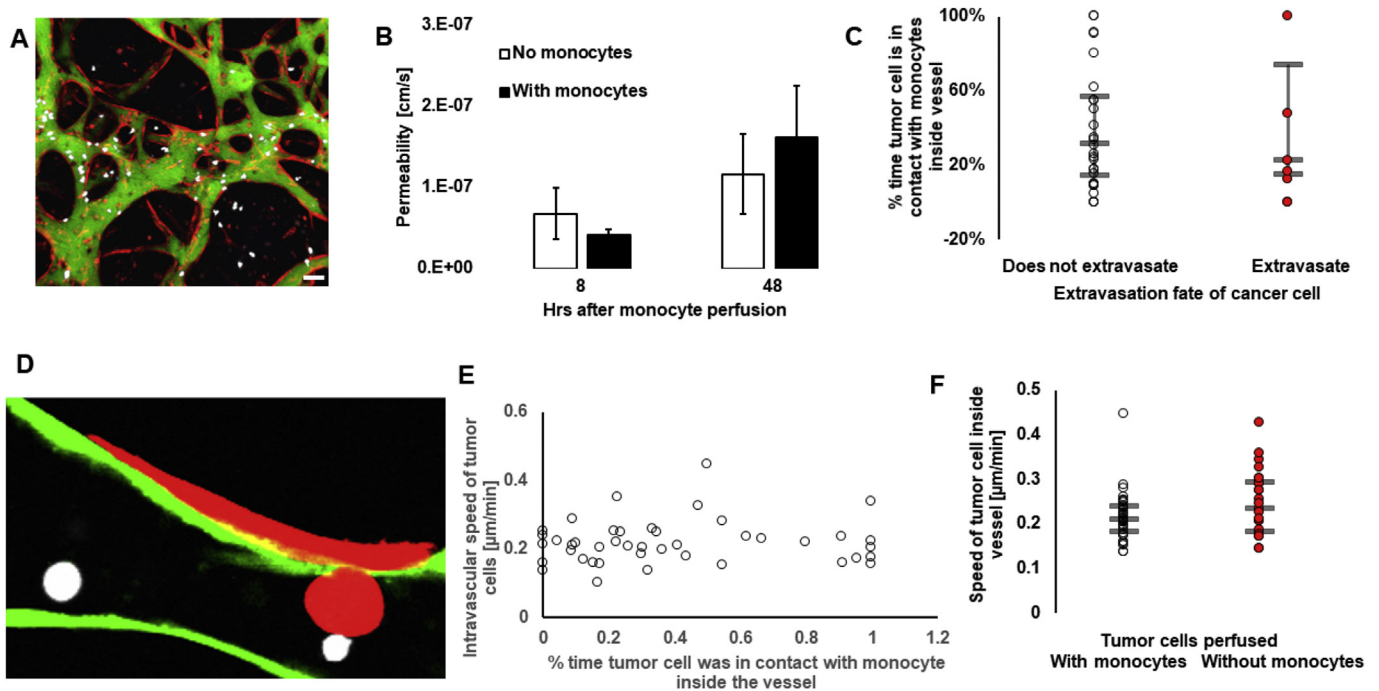
Fig. 7. Monocytes do not affect tumor cell extravasation in a contact-dependent manner. A) Confocal image of permeability measurements performed in the microvascular networks (red) using 70 kDa dextran (green) with monocytes (white), 8 h after monocyte perfusion in the networks. Bar is 30 μm. B) Quantification of the microvascular networks' average permeability in presence (filled bars) or absence (empty bars) of monocytes, 8 or 48 h after their perfusion in the assay. Bars are SEM. N = 3 donors per condition, N = 3–8 devices per condition. C) Percentage of time the tumor cell migrating inside the vessels were in contact with monocytes, grouped by their extravasation fate, i.e. for tumor cells that never extravasate (empty circles) or that eventually do (red circles). Each circle is a tumor cell. D) Confocal image showing a tumor cell (red) in direct contact with a monocyte (white) in the process of extravasating. Bar is 10 μm. E) Intravascular speed of tumor cells as a function of their average percentage time in contact with monocytes inside the vessels. Each circle represents a tumor cell. F) Speed of tumor cells migrating inside the vessels in assays where they have been perfused with (red circles) or without (empty circles) monocytes. Each circle represents a tumor cell. For C& E-F, the bars represent the third quartile, the median and first quartile of population.

macrophages [34]. Since we do observe an effect of blebbistatin on monocytes migrating on an endothelium, we speculate that adherence to the vessel wall might activate a myosin IIA requirement in monocytes.

Importantly, upregulation of macrophage-like markers on monocytes was reported in monocytes found in the extravascular space (Fig. 4E). In particular, we report the upregulation of CD68 that is a pan-macrophage marker and of CD163 [55] and CD206 that are two M2-like macrophage markers. This confirms that our system is powerful for studying monocyte-to-macrophage differentiation. An outstanding question in monocyte biology remains as to whether macrophage differentiation is directly linked to the process of extravasation itself. Indeed, studies have shown transmigration triggers changes in gene expression, such as downregulation of apoptotic genes [56], or genes associated with early monocyte to macrophage differentiation [57]. Our results suggest that monocyte differentiation occurs independently from extravasation since monocytes that did not extravasate also upregulated macrophage markers (Fig. 4E). Further study is needed to confirm this finding; however, our results suggest that the physical process of extravasation does not, alone, cause monocyte differentiation. Rather, micro-environmental factors derived from endothelial or other stromal cells would skew the monocytes phenotype, which agrees with other studies [58]. Interestingly, a study has shown that direct contact between endothelial cells and macrophages supports the survival of monocytes and skews their differentiation towards an M2 phenotype [59]. Note that this could also explain why many monocytes were found in our assay within 10–20 μm of the endothelial wall (Fig. 4B). More specifically they showed that CSF1 secretion by endothelia was responsible for the

macrophage colonies survival. We however did not detect any CSF1 secreted in media conditioned by fibroblasts or endothelial cells cultured in 2D (data not shown); while membrane bound CSF1 could be at play, we found that blocking CSF1 receptors with 2 μM of GW2580 did not significantly reduce the expression of CD206 in monocyte-derived macrophages (data not shown). Alternatively, it is known that monocytes spontaneously differentiate over time, upon adherence to 2D plates, but also that they can trigger their own differentiation via autocrine signaling, such as CXCL12 [60]. Blocking CXCL12 herein did not reduce the number of CD206 positive monocytes (data not shown). Importantly, our data examines the effect of extravasation on monocyte differentiation, but not the effect of embedding monocytes in a three-dimensional matrix. It is worth asking whether the stiffness of their local microenvironment, and their shape change in a 3D matrix partially explains their differentiation. The former idea is supported by a study that showed that macrophages grown on soft substrates produced less proinflammatory factors compared to macrophages placed on stiffer hydrogels [61]. The latter hypothesis is supported by a study that has shown that confining macrophages in 2D channels of varied size can polarize them towards distinct differentiation states [62]. While this could, in theory, have been tested in our experiment by comparing monocyte differentiation in 3D fibrin gels alone with monocytes in 2D, it was not carried out for two reasons: first, monocytes are hard to detach from well-plates to perform FACs analysis without affecting their viability or differentiation markers that lie on the surface. Second, viability of monocytes maintained alone in a 3D fibrin gel over several days drastically decreases (data not shown).

Finally, we exploit our system to explore how monocytes affect

cancer cell extravasation, as they would during metastasis. We first characterize tumor cell extravasation in our assay and show that extravasation is not dictated by the tumor cells' locomotive behavior inside the vasculature (Fig. 5B). While locomotion on an endothelium has been shown to be a crucial step during monocyte's extravasation to find the nearest junction [44], in our hands, the tumor cells that extravasate were not the ones that moved faster or that explored more of the vasculature (Fig. 5B/C). In addition, we show that tumor cells that are close to each other do not consistently choose to extravasate. Thus, we speculate that in our 3D assay, the extravasation potential of tumor cells is not simply dictated by local changes in the microvascular networks, but rather by a tumor cell's inherently variable potential for metastasis. Interestingly, some studies have suggested that cancer stem cells have enhanced invasive properties [63,64]. It was also shown that MDA-MB-231 contain a stem-cell like sub-population, although they did not seem to accelerate bone metastasis in mice compared to non-stemcell like MDA-MB-231 [65]. It is therefore possible that the sub-population of tumor cells that extravasate belong to CSC. This could be further studied in our system, by isolating cancer stem cell subpopulation and analyzing their extravasation rate compared to the non cancer stem cells. We then analyze tumor cell extravasation in presence of monocytes. Interestingly, we show that macrophage-like monocytes (following trans-endothelial migration), do not significantly affect the rate of cancer cell extravasation (Fig. 5F). This disagrees with in vivo studies that have shown that macrophage depletion leads to a drastic decrease in MDA-MB-231 in murine lungs within 24 h [15]. This discrepancy could arise from species-related differences (mouse versus human micro-environment) between our study and the aforementioned study; alternatively, it could be due to the fact that Qian. et al. examined resident alveolar macrophages whereas we studied inflammatory macrophages. Finally, we propose that our in vitro system is maybe missing important micro-environmental factors that are present in vivo to activate macrophages to engage with cancer cells especially in the metastatic niche. For example, CCL2 and CXCL12 are known to be important cytokines in the metastatic cascade [20,66], that can affect monocytes/macrophage recruitment and function [60,67]; while we did detect CCL2 being produced by both fibroblasts and endothelial cells, no CXCL12 was detectable (ELISAs, data not shown). Alternatively, maybe the effects become more obvious with longer-term survival. In any case, our data show that arrival of cancer cells to the secondary site alone is not enough to trigger an effect of macrophages on cancer cell extravasation.

Importantly, we report for the first time a monocyte-mediated effect on cancer cell extravasation. Specifically, we show that MDA-MB-231 extravasate less when perfused with monocytes. Preliminary data with MDA-MB-435 shows a similar trend. This has never been reported, notably because it is hard to replicate these experiments in conventional macroscopic in vitro systems or in vivo. We see that within 5 h, the presence of monocytes reduces the extravasation rate of MDA-MB-231 (Fig. 6C). Note that for these experiments, we perfused the whole population of monocytes isolated from human blood. Further studies should examine the potentially different roles of patrolling versus inflammatory monocytes have on cancer cells, especially since evidence suggests that they have different roles in cancer metastasis [1,20]. Of note, inflammatory monocytes have been shown to participate in promoting cancer metastasis only by replenishing the pool of macrophages into the tissue [20], i.e. after their trans-endothelial migration. Since we show that the bulk of the monocyte population in our experiments is made of inflammatory monocytes, our results suggest that they actually might have more of an anti-metastatic effect during their intra-vascular existence. Monocytes did not

affect the barrier properties of the endothelium (Fig. 7A/B), nor was the reduction in the extravasation of tumor cells contact-dependent (Fig. 7C). In other words, contact with monocytes did not directly inhibit cancer cell extravasation or affect their speed (Fig. 7C/E). Thus, we hypothesize that monocytes are affecting cancer cells in a paracrine fashion, which should be further investigated. Our qualitative results from the cytokine array we performed suggest that monocytes produce an important amount of CCL24, CCL2, CXCL7, GRO $_{a/b/g}$, IL-8, TIMP-1, TIMP-2 and some CCL5. While many of these have been associated to different cancers [18,38–41], only a few have been directly linked to cancer cell extravasation. However, both IL-8 [68] and CCL2 [69] were shown to increase cancer cell extravasation, contrary to the effect observed in this report. Interestingly, one study has shown that overexpression of TIMP-1 and TIMP-2 in a rat bladder carcinoma cell line diminished their extravasation in the lungs of mice. They hypothesized that the presence of these inhibitors of matrix metalloproteinases in the metastatic site prevented cancer cell from breaching the basement membrane and thus from extravasating [70]. If so, one could speculate that monocytes in producing these MMP inhibitors are preventing cancer cell extravasation in our assay. Yet, another study showed that over expressing TIMP-1 did not affect the extravasation of B16F10 in chick embryos but decreased their growth post-extravasation [71]. The role of TIMP-1 and TIMP-2 secreted by monocytes on cancer cell extravasation could therefore be further clarified in future studies using our system. In addition, we confirm that the decrease in tumor cell extravasation caused by signaling from monocytes is not caused by a change in the tumor cell intravascular locomotion (Fig. 7F). This lends support to the possibility that monocytes are preventing cancer cells from extravasating not by affecting their mobility but rather their ability to breach the basement membrane underlying endothelial cells, an important step in cancer cell extravasation [37,72,73]. Alternatively, the presence of monocytes might prevent tumor cell extravasation by altering the tumor cells' or local endothelial cells' surface-receptors, which have been shown to be important for achieving tumor [74] and leukocyte's [44] extravasation.

Taken together, our data brings to light a new role of monocytes in metastatic progression. This is the first study to report direct engagement of undifferentiated monocytes in tumor cell extravasation. Importantly, this study establishes a new and powerful 3D vascularized microfluidic model as a tool to study monocyte during intravascular and trans-endothelial migration, as well as in vivo-like differentiation. This platform promises to be a powerful model for screening drugs that can alter monocyte differentiation, which is a therapeutic avenue of interest to treat many diseases, including cancer. For example, anti-chemokine receptor antibodies could be tested to block chemokine-mediated monocyte differentiation or monocyte-cancer cell interactions. Other compounds could be tested, such as oligomeric proanthocyanidin complexes [75], vitamins [76], or chemotherapy [78], all of which have been shown to affect monocyte to macrophage differentiation. Future studies should include in this model flow which is known to be essential to monocytes homeostasis and their extravasation cascade. We also propose these studies should be repeated in presence of multiple immune cells, for example monocytes with platelets, as these are known to interact in the bloodstream especially for extravasation purpose [79]. Platelets have been shown to be important in the metastatic niche [80], therefore the synergistic effect of monocytes and platelets (or other immune cells) on tumor cells should be explored. Overall, our results warrant further in vitro and in vivo investigation into the role of monocytes in metastasis, in particular to screen for drugs that can potentiate the anti-metastatic effect observed in our assay.

Authors contributions

ABC performed and designed all experiments, and collected and analyzed all data (blood processing, microfluidic device fabrication, microvascular network formation, flow cytometry experiments, immunostaining, monocyte and cancer cell perfusion, confocal microscopy). YA made microfluidic devices, performed immuno-staining, helped with cell culture and analyzed data with Imaris. KH designed and performed permeability measurements experiments and analyzed the resulting data. MH and CL provided help with experimental design and data analysis. RDK provided supervision, helped design experiments and helped with data analysis. ABC wrote the manuscript, all authors reviewed and commented on the manuscript.

Acknowledgements

Appendix A. Supplementary data

Supplementary data related to this article can be found at https://doi.org/10.1016/j.biomaterials.2018.03.005.

References

[1] R.N. Hanna, et al., Patrolling monocytes control tumor metastasis to the lung 350 (6263) (2015) 985–991.

[2] K.J. Brempelis, I.N. Crispe, Infiltrating monocytes in liver injury and repair, Clin. Transl. Immunol. 5 (11) (Nov. 2016) e113.

[3] K. Grubczak, M. Monjuszko, The role of different monocyte subsets and macrophages in asthma pathogenesis, Prog Heal. Sci 5 (1) (2015) 176–184.

[4] F. Ginhoux, S. Jung, Monocytes and macrophages: developmental pathways and tissue homeostasis, Nat. Rev. Immunol. 14 (6) (Jun. 2014) 392–404.

[5] J. Yang, L. Zhang, C. Yu, X.-F. Yang, H. Wang, Monocyte and macrophage dif-ferentiation: circulation inflammatory monocyte as biomarker for inflamma-tory diseases, Biomark. Res. 2 (1) (2014) 1.

[6] S. Gordon, P.R. Taylor, Monocyte and macrophage heterogeneity, Nat. Rev. Immunol. 5 (12) (Dec. 2005) 953–964.

[7] A.A. Patel, et al., The fate and lifespan of human monocyte subsets in steady state and systemic inflammation, J. Exp. Med. 214 (7) (Jul. 2017) 1913–1923.

[8] G. Grage-Griebenow, H. Flad, M. Ernst, Heterogeneity of human peripheral blood monocyte subsets, J. Leukoc. Biol. 69 (1) (2001) 11–20.

[9] L.M. Carlin, et al., Nr4a1-dependent Ly6Clow monocytes monitor endothelial cells and orchestrate their disposal, Cell 153 (2) (2013) 362–375.

[10] A.D. Fesnak, C.H. June, B.L. Levine, Engineered T cells: the promise and chal-lenges of cancer immunotherapy, Nat. Rev. Cancer 16 (9) (Aug. 2016) 566–581.

[11] A. Mantovani, A. Vecchi, P. Allavena, Pharmacological modulation of mono-cytes and macrophages, Curr. Opin. Pharmacol. 17 (1) (2014) 38–44.

[12] T. Kitamura, B.-Z. Qian, J.W. Pollard, Immune cell promotion of metastasis, Nat. Rev. Immunol. 15 (2) (2015) 73–86.

[13] J.B. Wyckoff, J.G. Jones, J.S. Condeelis, J.E. Segall, A critical step in metastasis:

[14] J. Condeelis, J.W. Pollard, "Macrophages: obligate partners for tumor cell migration, invasion, and metastasis, Cell 124 (2) (Jan. 2006) 263–266.

[15] B. Qian, et al., A distinct macrophage population mediates metastatic breast cancer cell extravasation, establishment and growth, PLoS One 4 (8) (Jan. 2009) e6562.

[16] J. Wyckoff, et al., A paracrine loop between tumor cells and macrophages is required for tumor cell migration in mammary tumors, Cancer Res. 64 (19) (Oct. 2004) 7022–7029.

[17] B.-Z. Qian, J.W. Pollard, Macrophage diversity enhances tumor progression and metastasis, Cell 141 (1) (Apr. 2010) 39–51.

[18] T. Kitamura, et al., CCL2-induced chemokine cascade promotes breast cancer metastasis by enhancing retention of metastasis-associated macrophages, J. Exp. Med. 212 (7) (2015) 1043–1059.

[19] Q. Chen, X.H.-F. Zhang, J. Massagué, Macrophage binding to receptor VCAM-1 transmits survival signals in breast cancer cells that invade the lungs, Canc. Cell 20 (4) (Oct. 2011) 538–549.

[20] B.-Z. Qian, et al., CCL2 recruits inflammatory monocytes to facilitate breast-tumour metastasis, Nature 475 (7355,) (Jul. 2011) 222–225.

[21] K.L. Butler, E. Clancy-Thompson, D.W. Mullins, CXCR3+ monocytes/macro-phages are required for establishment of pulmonary metastases, Sci. Rep. 7 (Mar. 2017) 45593.

[22] E. Sahai, Illuminating the metastatic process, Nat. Rev. Cancer 7 (10) (Oct. 2007) 737–749.

[23] A. Boussommier-calleja, R. Li, M.B. Chen, S.C. Wong, R.D. Kamm, Microfluidics: a new tool for modeling cancer − immune interactions, Trends Cancer 2 (1) (2016) 6–19.

[24] G.M. Whitesides, "The origins and the future of microfluidics, Nature 442 (7101) (2006) 368–373.

[25] M. Junkin, S. Tay, Microfluidic single-cell analysis for systems immunology, Lab a Chip 14 (7) (2014) 1246–1260.

[26] J.A. Whisler, M.B. Chen, R.D. Kamm, Control of perfusable microvascular network morphology using a multiculture microfluidic system, Tissue Eng. Part C Methods 20 (7) (Jul. 2014) 543–552.

[27] J.H. Yeon, H.R. Ryu, M. Chung, Q.P. Hu, N.L. Jeon, In vitro formation and characterization of a perfusable three-dimensional tubular capillary network in microfluidic devices, Lab a Chip 12 (16) (Aug. 2012) 2815–2822.

[28] M.B. Chen, J.A. Whisler, J. Fröse, C. Yu, Y. Shin, R.D. Kamm, On-chip human microvasculature assay for visualization and quantification of tumor cell extravasation dynamics, Nat. Protoc. 12 (5) (2017) 865–880.

[29] B. Carrion, I.A. Janson, Y.P. Kong, A.J. Putnam, A safe and efficient method to retrieve mesenchymal stem cells from three-dimensional fibrin gels, Tissue Eng. Part C Methods 20 (3) (Mar. 2014) 252–263.

[30] S. Kim, H. Lee, M. Chung, N.L. Jeon, "Engineering of functional, perfusable 3D microvascular networks on a chip, Lab. Chip. 13 (8) (2013) 1489–1500.

[31] T. Silzle, M. Kreutz, M.A. Dobler, G. Brockhoff, R. Knuechel, L.A. Kunz-Schughart, "Tumor-associated fibroblasts recruit blood monocytes into tumor tissue, Eur. J. Immunol. 33 (5) (2003) 1311–1320.

[32] C. Shi, E.G. Pamer, "Monocyte recruitment during infection and inflammation, Nat. Rev. Immunol. 11 (11) (2011) 762–774.

[33] K.M. Stroka, H.N. Hayenga, H. Aranda-Espinoza, Human neutrophil cytoskel-etal dynamics and contractility actively contribute to trans-endothelial migration, PLoS One 8 (no. 4) (2013).

[34] C.J. Chan, et al., Myosin II activity softens cells in suspension, Biophys. J. 108 (8) (2015) 1856–1869.

[35] L.E. Hind, M. Dembo, D.A. Hammer, Macrophage motility is driven by frontal-towing with a force magnitude dependent on substrate stiffness, Integr. Biol. Camb. 7 (4) (Apr. 2015) 447–453.

[36] J. Jacobelli, et al., Confinement-optimized three-dimensional T cell amoeboid motility is modulated via myosin IIA−regulated adhesions, Nat. Immunol. 11 (10) (Oct. 2010) 953–961.

[37] M.B. Chen, J.A. Whisler, J.S. Jeon, R.D. Kamm, Mechanisms of tumor cell extravasation in an in vitro microvascular network platform, Integr. Biol. Camb 5 (10) (Oct. 2013) 1262–1271.

[38] D.J.J. Waugh, C. Wilson, The interleukin-8 pathway in cancer, Clin. Cancer Res. 14 (21) (Nov. 2008) 6735–6741.

[39] S. Lian, et al., Elevated expression of growth-regulated oncogene-alpha in tumor and stromal cells predicts unfavorable prognosis in pancreatic cancer, Med. Baltimore. 95 (30) (Jul. 2016) e4328.

[40] T. Desurmont, et al., Overexpression of chemokine receptor CXCR2 and ligand CXCL7 in liver metastases from colon cancer is correlated to shorter disease-free and overall survival, Cancer Sci. 106 (3) (Mar. 2015) 262–269.

[41] L. Jin, et al., CCL24 contributes to HCC malignancy via RhoB- VEGFA-VEGFR2 angiogenesis pathway and indicates poor prognosis, Oncotarget 8 (3) (Jan. 2017) 402–406.

[42] C. Auffray, et al., Monitoring of blood vessels and tissues by a population of monocytes with patrolling behavior 317 (August) (2007) 666–671.

[43] J.B. Wyckoff, et al., Direct visualization of macrophage-assisted tumor cell intravasation in mammary tumors, Cancer Res. 67 (6) (Mar. 2007) 2649–2656.

[44] A.R. Schenkel, Z. Mamdouh, W.A. Muller, Locomotion of monocytes on endothelium is a critical step during extravasation, Nat. Immunol. 5 (4) (2004) 393–400.

[45] A.R. Schenkel, Z. Mamdouh, X. Chen, R.M. Liebman, W.A. Muller, CD99 plays a

major role in the migration of monocytes through endothelial junctions, Nat. Immunol. 3 (2) (Feb. 2002) 143–150.

[46] K. Haase, R.D. Kamm, Advances in on-chip vascularization, Regen. Med. 12 (3) (Apr. 2017) 285–302.

[47] J.L. Collison, L.M. Carlin, M. Eichmann, F. Geissmann, M. Peakman, Heterogeneity in the locomotory behavior of human monocyte subsets over human vascular endothelium in vitro, J. Immunol. 195 (3) (2015) 1162–1170.

[48] T. Gerhardt, K. Ley, Monocyte trafficking across the vessel wall, Cardiovasc. Res. 107 (3) (2015) 321–330.

[49] J. Cros, et al., Human CD14dim monocytes patrol and sense nucleic acids and viruses via TLR7 and TLR8 receptors, Immunity 33 (3) (2010) 375–386.

[50] C.-L. Tsou, et al., Critical roles for CCR2 and MCP-3 in monocyte mobilization from bone marrow and recruitment to inflammatory sites, J. Clin. Invest. 117 (4) (Apr. 2007) 902–909.

[51] G. Thomas, R. Tacke, C.C. Hedrick, R.N. Hanna, Nonclassical patrolling monocyte function in the vasculature, Arterioscler. Thromb. Vasc. Biol. 35 (6) (2015) 1306–1316.

[52] J. Jacobelli, M. Estin Matthews, S. Chen, M.F. Krummel, Activated T cell transendothelial migration relies on myosin-IIA contractility for squeezing the cell nucleus through endothelial cell barriers, PLoS One 8 (9) (2013) 1–13.

[53] J. Si, Y. Ge, S. Zhuang, R. Gong, Inhibiting nonmuscle myosin II impedes inflammatory infiltration and ameliorates progressive renal disease, Lab. Invest. 90 (3) (2010) 448–458.

[54] R. Bzymek, et al., Real-time two- and three-dimensional imaging of monocyte motility and navigation on planar surfaces and in collagen matrices: roles of Rho, Sci. Rep. 6 (February) (2016) 25016.

[55] M.H.M. Barros, F. Hauck, J.H. Dreyer, B. Kempkes, G. Niedobitek, Macrophage polarisation: an immunohistochemical approach for identifying M1 and M2 macrophages, PLoS One 8 (11) (Nov. 2013) e80908.

[56] M.R. Williams, Y. Sakurai, S.M. Zughaier, S.G. Eskin, L.V. McIntire, Transmigration across activated endothelium induces transcriptional changes, inhibits apoptosis, and decreases antimicrobial protein expression in human monocytes, J. Leukoc. Biol. 86 (6) (Dec. 2009) 1331–1343.

[57] S. Ghavampour, C. Lange, C. Bottino, V. Gerke, Transcriptional profiling of human monocytes identifies the inhibitory receptor CD300a as regulator of transendothelial migration, PLoS One 8 (9) (2013).

[58] P. Italiani, D. Boraschi, From monocytes to m1/m2 macrophages: phenotypical vs. Functional differentiation, Front. Immunol. 5 (Oct. 2014).

[59] H. He, et al., Endothelial cells provide an instructive niche for the differentiation and functional polarization of M2-like macrophages, Blood 120 (15) (Oct. 2012) 3152–3162.

[60] L. Sánchez-Martín, A. Estecha, R. Samaniego, S. Sánchez-Ramón, M.Á. Vega, P. Sánchez-Mateos, The chemokine CXCL12 regulates monocyte-macrophage differentiation and RUNX3 expression, Blood 117 (1) (2011) 88–97.

[61] M.L. Previtera, A. Sengupta, Substrate stiffness regulates proinflammatory mediator production through TLR4 activity in macrophages, PLoS One 10 (12) (Dec. 2015) e0145813.

[62] F.Y. McWhorter, T. Wang, P. Nguyen, T. Chung, W.F. Liu, Modulation of macrophage phenotype by cell shape, Proc. Natl. Acad. Sci. Unit. States Am. 110 (43) (2013) 17253–17258.

[63] E. Charafe-Jauffret, et al., Breast cancer cell lines contain functional cancer stem cells with metastatic capacity and a distinct molecular signature, Cancer Res 69 (4) (Feb. 2009) 1302–1313.

[64] C. Sheridan, et al., CD44+/CD24- breast cancer cells exhibit enhanced invasive properties: an early step necessary for metastasis, Breast Cancer Res. 8 (5) (2006) R59.

[65] T. Hiraga, S. Ito, H. Nakamura, Side population in MDA-MB-231 human breast cancer cells exhibits cancer stem cell-like properties without higher bone-metastatic potential, Oncol. Rep. 25 (1) (Jan. 2011) 289–296.

[66] S. Cavallaro, CXCR4/CXCL12 in non-small-cell lung cancer metastasis to the brain, Int. J. Mol. Sci. 14 (1) (Jan. 2013) 1713–1727.

[67] E. Sierra-Filardi, et al., CCL2 shapes macrophage polarization by GM-CSF and M-CSF: identification of CCL2/CCR2-dependent gene expression profile, J. Immunol. 192 (8) (2014) 3858–3867.

[68] Y.S. Lee, et al., Interleukin-8 and its receptor CXCR2 in the tumour microenvironment promote colon cancer growth, progression and metastasis, Br. J. Cancer 106 (11) (May 2012) 1833–1841.

[69] M.J. Wolf, et al., Endothelial CCR2 signaling induced by colon carcinoma cells enables extravasation via the JAK2-Stat5 and p38MAPK pathway, Canc. Cell 22 (1) (Jul. 2012) 91–105.

[70] H. Kawamata, K. Kawai, S. Kameyama, M.D. Johnson, W.G. Stetler-Stevenson, R. Oyasu, Over-expression of tissue inhibitor of matrix metalloproteinases (TIMP1 and TIMP2) suppresses extravasation of pulmonary metastasis of a rat bladder carcinoma, Int. J. Cancer 63 (5) (1995) 680–687.

[71] S. Koop, et al., Overexpression of Metalloproteinase Inhibitor in B16F10 Cells Does Not Affect Extravasation but Reduces Tumor Growth Overexpression of Metalloproteinase Inhibitor in B16F10 Cells Does Not Affect Extravasation but Reduces Tumor Growth1, 1994, pp. 4791–4797.

[72] K. Stoletov, V. Montel, R.D. Lester, S.L. Gonias, R. Klemke, High-resolution imaging of the dynamic tumor cell vascular interface in transparent zebrafish, Proc. Natl. Acad. Sci. Unit. States Am. 104 (44) (Oct. 2007) 17406–17411.

[73] H.S. Leong, et al., Invadopodia are required for cancer cell extravasation and are a therapeutic target for metastasis, Cell Rep. 8 (5) (2014) 1558–1570.

[74] C.T. Mierke, "Role of the endothelium during tumor cell metastasis: is the endothelium a barrier or a promoter for cell invasion and metastasis? J. Biophys. 2008 (2008), 183516.

[75] T. Mohana, A.V. Navin, S. Jamuna, M.S. Sakeena Sadullah, S. Niranjali Devaraj, Inhibition of differentiation of monocyte to macrophages in atherosclerosis by oligomeric proanthocyanidins -In-vivo and in-vitro study, Food Chem. Toxicol. 82 (Aug. 2015) 96–105.

[76] R. Weiss, et al., Nicotinamide: a vitamin able to shift macrophage differentiation toward macrophages with restricted inflammatory features, Innate Immun. 21 (8) (Nov. 2015) 813–826.

[78] E.M. Dijkgraaf, et al., Chemotherapy alters monocyte differentiation to favor generation of cancer-supporting M2 macrophages in the tumor microenvironment, Cancer Res 73 (8) (Apr. 2013) 2480–2492.

[79] J.B. Kral, W.C. Schrottmaier, M. Salzmann, A. Assinger, Platelet interaction with innate immune cells, Transfus. Med. Hemotherapy 43 (2) (Mar. 2016) 78–88.

[80] M. Labelle, S. Begum, R.O. Hynes, Platelets guide the formation of early metastatic niches, Proc. Natl. Acad. Sci. U. S. A. 111 (30) (2014) 3053–3061.